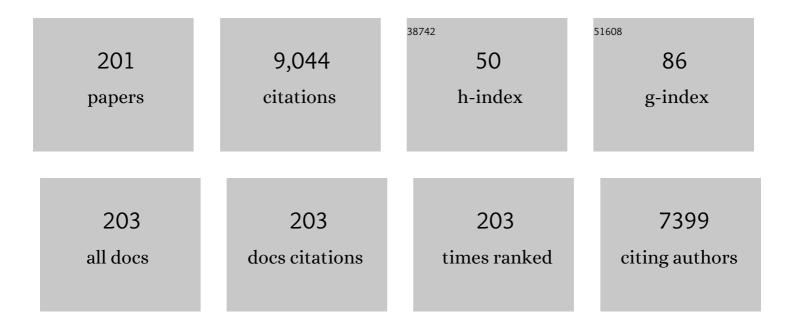
List of Publications by Year in descending order

Source: https://exaly.com/author-pdf/2672750/publications.pdf Version: 2024-02-01



#	Article	IF	CITATIONS
1	Cu2ZnSnS4 solar cells with over 10% power conversion efficiency enabled by heterojunction heat treatment. Nature Energy, 2018, 3, 764-772.	39.5	623
2	MoS ₂ Nanosheets: A Designed Structure with High Active Site Density for the Hydrogen Evolution Reaction. ACS Catalysis, 2013, 3, 2101-2107.	11.2	340
3	Over 9% Efficient Kesterite Cu ₂ ZnSnS ₄ Solar Cell Fabricated by Using Zn _{1–} <i>_x</i> Cd <i>_x</i> S Buffer Layer. Advanced Energy Materials, 2016, 6, 1600046.	19.5	322
4	The current status and future prospects of kesterite solar cells: a brief review. Progress in Photovoltaics: Research and Applications, 2016, 24, 879-898.	8.1	316
5	Fabrication of Cu ₂ ZnSnS ₄ solar cells with 5.1% efficiency via thermal decomposition and reaction using a non-toxic sol–gel route. Journal of Materials Chemistry A, 2014, 2, 500-509.	10.3	249
6	Beyond 11% Efficient Sulfide Kesterite Cu ₂ Zn _{<i>x</i>} Cd _{1–<i>x</i>} SnS ₄ Solar Cell: Effects of Cadmium Alloying. ACS Energy Letters, 2017, 2, 930-936.	17.4	249
7	Device Postannealing Enabling over 12% Efficient Solutionâ€Processed Cu ₂ ZnSnS ₄ Solar Cells with Cd ²⁺ Substitution. Advanced Materials, 2020, 32, e2000121.	21.0	201
8	In situ growth of Cu2ZnSnS4 thin films by reactive magnetron co-sputtering. Solar Energy Materials and Solar Cells, 2010, 94, 2431-2434.	6.2	200
9	Characterization of chemical bath deposited CdS thin films at different deposition temperature. Journal of Alloys and Compounds, 2010, 493, 305-308.	5.5	200
10	Band alignments of different buffer layers (CdS, Zn(O,S), and In2S3) on Cu2ZnSnS4. Applied Physics Letters, 2014, 104, .	3.3	148
11	Fabrication of ternary Cu–Sn–S sulfides by a modified successive ionic layer adsorption and reaction (SILAR) method. Journal of Materials Chemistry, 2012, 22, 16346.	6.7	141
12	Synthesis and characterizations of quaternary Cu2FeSnS4 nanocrystals. Chemical Communications, 2012, 48, 2603.	4.1	137
13	Defect Control for 12.5% Efficiency Cu ₂ ZnSnSe ₄ Kesterite Thinâ€Film Solar Cells by Engineering of Local Chemical Environment. Advanced Materials, 2020, 32, e2005268.	21.0	133
14	Enhancing the Cu2ZnSnS4 solar cell efficiency by back contact modification: Inserting a thin TiB2 intermediate layer at Cu2ZnSnS4/Mo interface. Applied Physics Letters, 2014, 104, .	3.3	131
15	Integrated Photorechargeable Energy Storage System: Nextâ€Generation Power Source Driving the Future. Advanced Energy Materials, 2020, 10, 1903930.	19.5	128
16	Beyond 8% ultrathin kesterite Cu2ZnSnS4 solar cells by interface reaction route controlling and self-organized nanopattern at the back contact. NPG Asia Materials, 2017, 9, e401-e401.	7.9	118
17	Polytype 1T/2H MoS2 heterostructures for efficient photoelectrocatalytic hydrogen evolution. Chemical Engineering Journal, 2017, 330, 102-108.	12.7	116
18	Boosting Cu2ZnSnS4 solar cells efficiency by a thin Ag intermediate layer between absorber and back contact. Applied Physics Letters, 2014, 104, .	3.3	113

#	Article	IF	CITATIONS
19	Nanoscale Microstructure and Chemistry of Cu ₂ ZnSnS ₄ /CdS Interface in Kesterite Cu ₂ ZnSnS ₄ Solar Cells. Advanced Energy Materials, 2016, 6, 1600706.	19.5	113
20	Effects of potassium doping on solution processed kesterite Cu2ZnSnS4 thin film solar cells. Applied Physics Letters, 2014, 105, .	3.3	101
21	Boosting the efficiency of pure sulfide CZTS solar cells using the In/Cd-based hybrid buffers. Solar Energy Materials and Solar Cells, 2016, 144, 700-706.	6.2	101
22	Perovskite-based tandem solar cells. Science Bulletin, 2021, 66, 621-636.	9.0	91
23	Sulfur vacancy engineering of MoS2 via phosphorus incorporation for improved electrocatalytic N2 reduction to NH3. Applied Catalysis B: Environmental, 2022, 300, 120733.	20.2	85
24	Emerging inorganic compound thin film photovoltaic materials: Progress, challenges and strategies. Materials Today, 2020, 41, 120-142.	14.2	81
25	Nucleation and growth of selenium electrodeposition onto tin oxide electrode. Journal of Electroanalytical Chemistry, 2010, 639, 187-192.	3.8	80
26	Cyclic voltammetry study of electrodeposition of Cu(In,Ga)Se2 thin films. Electrochimica Acta, 2009, 54, 3004-3010.	5.2	79
27	Preparation and characterization of Sb2Se3 thin films by electrodeposition and annealing treatment. Applied Surface Science, 2012, 261, 510-514.	6.1	79
28	Improvement of <i>J</i> _{sc} in a Cu ₂ ZnSnS ₄ Solar Cell by Using a Thin Carbon Intermediate Layer at the Cu ₂ ZnSnS ₄ /Mo Interface. ACS Applied Materials & Interfaces, 2015, 7, 22868-22873.	8.0	78
29	Inhibiting MoS2 formation by introducing a ZnO intermediate layer for Cu2ZnSnS4 solar cells. Materials Letters, 2014, 130, 87-90.	2.6	76
30	A two-terminal all-inorganic perovskite/organic tandem solar cell. Science Bulletin, 2019, 64, 885-887.	9.0	76
31	An alternative route towards low-cost Cu2ZnSnS4 thin film solar cells. Surface and Coatings Technology, 2013, 232, 53-59.	4.8	74
32	Characterization of nano-lead-doped active carbon and its application in lead-acid battery. Journal of Power Sources, 2014, 270, 332-341.	7.8	72
33	Kesterite Cu ₂ ZnSn(S,Se) ₄ Solar Cells with beyond 8% Efficiency by a Sol–Gel and Selenization Process. ACS Applied Materials & Interfaces, 2015, 7, 14376-14383.	8.0	72
34	The Role of Hydrogen from ALDâ€Al ₂ O ₃ in Kesterite Cu ₂ ZnSnS ₄ Solar Cells: Grain Surface Passivation. Advanced Energy Materials, 2018, 8, 1701940.	19.5	68
35	Solution-based synthesis of chalcostibite (CuSbS2) nanobricks for solar energy conversion. RSC Advances, 2012, 2, 10481.	3.6	67
36	Enhanced Heterojunction Interface Quality To Achieve 9.3% Efficient Cd-Free Cu ₂ ZnSnS ₄ Solar Cells Using Atomic Layer Deposition ZnSnO Buffer Layer. Chemistry of Materials, 2018, 30, 7860-7871.	6.7	66

#	Article	IF	CITATIONS
37	Synthesis and characterization of multicomponent Cu2(FexZn1â^'x)SnS4 nanocrystals with tunable band gap and structure. Journal of Materials Chemistry A, 2013, 1, 5402.	10.3	65
38	Boost Voc of pure sulfide kesterite solar cell via a double CZTS layer stacks. Solar Energy Materials and Solar Cells, 2017, 160, 7-11.	6.2	65
39	Photoelectrochemical Determination of Cu ²⁺ Using a WO ₃ /CdS Heterojunction Photoanode. ACS Applied Materials & Interfaces, 2019, 11, 37541-37549.	8.0	65
40	Fabrication of Sb2S3 thin films by sputtering and post-annealing for solar cells. Ceramics International, 2019, 45, 3044-3051.	4.8	64
41	Preparation of Cu2ZnSnS4 thin films by sulfurizing stacked precursor thin films via successive ionic layer adsorption and reaction method. Applied Surface Science, 2012, 258, 7678-7682.	6.1	63
42	CsPbI2.25Br0.75 solar cells with 15.9% efficiency. Science Bulletin, 2019, 64, 507-510.	9.0	62
43	Kesterite Cu ₂ ZnSnS ₄ thin film solar cells by a facile DMF-based solution coating process. Journal of Materials Chemistry C, 2015, 3, 10783-10792.	5.5	61
44	Enhanced photoelectrochemical degradation of tetracycline hydrochloride with FeOOH and Au nanoparticles decorated WO3. Chemical Engineering Journal, 2021, 407, 127195.	12.7	59
45	Colloidal synthesis and characterizations of wittichenite copper bismuth sulphide nanocrystals. Nanoscale, 2013, 5, 1789.	5.6	55
46	Preparation and characterization of a novel and recyclable InVO4/ZnFe2O4 composite for methylene blue removal by adsorption and visible-light photocatalytic degradation. Applied Surface Science, 2020, 501, 144006.	6.1	55
47	Modification of absorber quality and Mo-back contact by a thin Bi intermediate layer for kesterite Cu2ZnSnS4 solar cells. Solar Energy Materials and Solar Cells, 2016, 144, 537-543.	6.2	54
48	Solution-Processed Trigonal Cu ₂ BaSnS ₄ Thin-Film Solar Cells. ACS Applied Energy Materials, 2018, 1, 3420-3427.	5.1	54
49	In situ growth of SnS absorbing layer by reactive sputtering for thin film solar cells. RSC Advances, 2016, 6, 4108-4115.	3.6	53
50	Efficiency Enhancement of Kesterite Cu ₂ ZnSnS ₄ Solar Cells via Solution-Processed Ultrathin Tin Oxide Intermediate Layer at Absorber/Buffer Interface. ACS Applied Energy Materials, 2018, 1, 154-160.	5.1	53
51	Fabrication of Cu ₂ ZnSnS ₄ nanowires and nanotubes based on AAO templates. CrystEngComm, 2012, 14, 782-785.	2.6	50
52	Hydrogen evolution inhibition with diethylenetriamine modification of activated carbon for a lead-acid battery. RSC Advances, 2014, 4, 33574-33577.	3.6	50
53	Quasi-Vertically-Orientated Antimony Sulfide Inorganic Thin-Film Solar Cells Achieved by Vapor Transport Deposition. ACS Applied Materials & Interfaces, 2020, 12, 22825-22834.	8.0	50
54	Flexible kesterite Cu2ZnSnS4 solar cells with sodium-doped molybdenum back contacts on stainless steel substrates. Solar Energy Materials and Solar Cells, 2018, 182, 14-20.	6.2	49

#	Article	IF	CITATIONS
55	Advances in kesterite Cu2ZnSn(S, Se)4 solar cells. Science Bulletin, 2020, 65, 698-701.	9.0	49
56	Improving Cu ₂ ZnSnS ₄ (CZTS) solar cell performance by an ultrathin ZnO intermediate layer between CZTS absorber and Mo back contact. Physica Status Solidi - Rapid Research Letters, 2014, 8, 966-970.	2.4	48
57	Influence of sodium incorporation on kesterite Cu2ZnSnS4 solar cells fabricated on stainless steel substrates. Solar Energy Materials and Solar Cells, 2016, 157, 565-571.	6.2	48
58	Growth and Characterization of Cu[sub 2]ZnSnS[sub 4] Thin Films by DC Reactive Magnetron Sputtering for Photovoltaic Applications. Electrochemical and Solid-State Letters, 2010, 13, H379.	2.2	46
59	MoS ₂ nanodot decorated In ₂ S ₃ nanoplates: a novel heterojunction with enhanced photoelectrochemical performance. Chemical Communications, 2016, 52, 1867-1870.	4.1	46
60	Beyond 10% efficiency Cu ₂ ZnSnS ₄ solar cells enabled by modifying the heterojunction interface chemistry. Journal of Materials Chemistry A, 2019, 7, 27289-27296.	10.3	46
61	Porous Heteroatom-Doped Ti ₃ C ₂ T _{<i>x</i>} MXene Microspheres Enable Strong Adsorption of Sodium Polysulfides for Long-Life Room-Temperature Sodium–Sulfur Batteries. ACS Nano, 2021, 15, 16207-16217.	14.6	46
62	Growth and characterization of CuSbSe2 thin films prepared by electrodeposition. Electrochimica Acta, 2012, 76, 480-486.	5.2	45
63	Novel phosphorus-doped PbO2–MnO2 bicontinuous electrodes for oxygen evolution reaction. RSC Advances, 2014, 4, 24020.	3.6	43
64	Construction of In2Se3/MoS2 heterojunction as photoanode toward efficient photoelectrochemical water splitting. Chemical Engineering Journal, 2019, 358, 752-758.	12.7	42
65	Epitaxial Cu2ZnSnS4 thin film on Si (111) 4° substrate. Applied Physics Letters, 2015, 106, .	3.3	41
66	Electrodeposition of Cobalt Selenide Thin Films. Journal of the Electrochemical Society, 2010, 157, D523.	2.9	40
67	Improving the conversion efficiency of Cu2ZnSnS4 solar cell by low pressure sulfurization. Applied Physics Letters, 2014, 104, .	3.3	40
68	Efficient Planar Perovskite Solar Cells with Reduced Hysteresis and Enhanced Open Circuit Voltage by Using PW ₁₂ –TiO ₂ as Electron Transport Layer. ACS Applied Materials & Interfaces, 2016, 8, 8520-8526.	8.0	40
69	Flexible Cu ₂ ZnSnS ₄ solar cells based on successive ionic layer adsorption and reaction method. RSC Advances, 2014, 4, 17703-17708.	3.6	39
70	Colloidal synthesis and characterisation of Cu ₃ SbSe ₃ nanocrystals. Journal of Materials Chemistry A, 2014, 2, 6363-6367.	10.3	38
71	Characterization of porous bismuth oxide (Bi ₂ O ₃) nanoplates prepared by chemical bath deposition and post annealing. RSC Advances, 2015, 5, 65591-65594.	3.6	38
72	Self-assembled Nanometer-Scale ZnS Structure at the CZTS/ZnCdS Heterointerface for High-Efficiency Wide Band Gap Cu ₂ ZnSnS ₄ Solar Cells. Chemistry of Materials, 2018, 30, 4008-4016.	6.7	37

#	Article	IF	CITATIONS
73	Electrodeposition of antimony selenide thin films from aqueous acid solutions. Journal of Electroanalytical Chemistry, 2012, 671, 73-79.	3.8	35
74	Photoelectrochemically deposited Sb ₂ Se ₃ thin films: deposition mechanism and characterization. RSC Advances, 2015, 5, 85592-85597.	3.6	35
75	Simulation and parameter identification based on electrochemical- thermal coupling model of power lithium ion-battery. Journal of Alloys and Compounds, 2020, 844, 156003.	5.5	35
76	Preparation of Cu(In,Ca)Se2 thin films by pulse electrodeposition. Journal of Alloys and Compounds, 2011, 509, L129-L133.	5.5	34
77	The effect of thermal evaporated MoO3 intermediate layer as primary back contact for kesterite Cu2ZnSnS4 solar cells. Thin Solid Films, 2018, 648, 39-45.	1.8	34
78	Photoelectrochemical properties of Bi 2 S 3 thin films deposited by successive ionic layer adsorption and reaction (SILAR) method. Journal of Alloys and Compounds, 2016, 686, 684-692.	5.5	33
79	Electrodeposition and characterization of copper bismuth selenide semiconductor thin films. Electrochimica Acta, 2013, 87, 153-157.	5.2	32
80	Growth and characterization of Cu2ZnSnS4 photovoltaic thin films by electrodeposition and sulfurization. Journal of Alloys and Compounds, 2014, 610, 331-336.	5.5	32
81	Exploring the application of metastable wurtzite nanocrystals in pure-sulfide Cu ₂ ZnSnS ₄ solar cells by forming nearly micron-sized large grains. Journal of Materials Chemistry A, 2015, 3, 23185-23193.	10.3	32
82	Understanding the Key Factors of Enhancing Phase and Compositional Controllability for 6% Efficient Pure-Sulfide Cu ₂ ZnSnS ₄ Solar Cells Prepared from Quaternary Wurtzite Nanocrystals. Chemistry of Materials, 2016, 28, 3649-3658.	6.7	32
83	Stable alkali metal anodes enabled by crystallographic optimization – a review. Journal of Materials Chemistry A, 2021, 9, 20957-20984.	10.3	32
84	Insights on the Properties of the O-Doped Argyrodite Sulfide Solid Electrolytes (Li ₆ PS _{5–<i>x</i>/sub>ClO_{<i>x</i>,} <i>x</i>=O–1). ACS Applied Materials & Interfaces, 2021, 13, 54924-54935.}	8.0	32
85	Minority lifetime and efficiency improvement for CZTS solar cells via Cd ion soaking and post treatment. Journal of Alloys and Compounds, 2018, 750, 328-332.	5.5	31
86	Highly Efficient Electrocatalytic N ₂ Reduction to Ammonia over Metallic 1T Phase of MoS ₂ Enabled by Active Sites Separation Mechanism. Advanced Science, 2022, 9, e2103583.	11.2	31
87	Effects of sodium sulfamate on electrodeposition of Cu(In,Ga)Se2 thin film. Journal of Electroanalytical Chemistry, 2011, 651, 191-196.	3.8	30
88	Bioinspired fiber-like porous Cu/N/C electrocatalyst facilitating electron transportation toward oxygen reaction for metal–air batteries. Nanoscale, 2018, 10, 15819-15825.	5.6	30
89	Kesterite Cu2ZnSnS4 solar cell from sputtered Zn/(Cu & Sn) metal stack precursors. Journal of Alloys and Compounds, 2014, 610, 486-491.	5.5	29
90	Highly efficient perovskite solar cells with precursor composition-dependent morphology. Solar Energy Materials and Solar Cells, 2016, 145, 231-237.	6.2	29

#	Article	IF	CITATIONS
91	A Stable and Efficient Photocathode Using an Sb ₂ S ₃ Absorber in a Near-Neutral Electrolyte for Water Splitting. ACS Applied Energy Materials, 2020, 3, 6188-6194.	5.1	29
92	Incorporation Mechanism of Indium and Gallium during Electrodeposition of Cu(In,Ga)Se2 Thin Film. Journal of the Electrochemical Society, 2011, 158, D704.	2.9	27
93	Platelike WO3 from hydrothermal RF sputtered tungsten thin films for photoelectrochemical water oxidation. Materials Letters, 2012, 84, 41-43.	2.6	27
94	Boosting the kesterite Cu2ZnSnS4 solar cells performance by diode laser annealing. Solar Energy Materials and Solar Cells, 2018, 175, 71-76.	6.2	27
95	Ambient air-processed Cu2ZnSn(S,Se)4 solar cells with over 12% efficiency. Science Bulletin, 2021, 66, 880-883.	9.0	27
96	One-Step Electrodeposition and Annealing of CuSbSe2 Thin Films. Electrochemical and Solid-State Letters, 2011, 15, D11-D13.	2.2	26
97	Fabrication of pyrite FeS2 thin films by sulfurizing oxide precursor films deposited via successive ionic layer adsorption and reaction method. Thin Solid Films, 2013, 542, 123-128.	1.8	26
98	High openâ€circuit voltage CuSbS ₂ solar cells achieved through the formation of epitaxial growth of CdS/CuSbS ₂ heteroâ€interface by postâ€annealing treatment. Progress in Photovoltaics: Research and Applications, 2019, 27, 37-43.	8.1	26
99	Reductive acid leaching of valuable metals from spent lithium-ion batteries using hydrazine sulfate as reductant. Transactions of Nonferrous Metals Society of China, 2020, 30, 2256-2264.	4.2	26
100	A two-dimension laminar composite protective layer for dendrite-free lithium metal anode. Journal of Energy Chemistry, 2021, 56, 391-394.	12.9	26
101	In situ growth of Sb 2 S 3 thin films by reactive sputtering on n-Si(100) substrates for top sub-cell of silicon based tandem solar cells. Materials Letters, 2017, 195, 186-189.	2.6	25
102	Rapid thermal annealed Molybdenum back contact for Cu2ZnSnS4 thin film solar cells. Applied Physics Letters, 2015, 106, .	3.3	24
103	Preparation and characterization of Bi-doped antimony selenide thin films by electrodeposition. Electrochimica Acta, 2011, 56, 8597-8602.	5.2	23
104	Low-Temperature Solution Processed Random Silver Nanowire as a Promising Replacement for Indium Tin Oxide. ACS Applied Materials & Interfaces, 2017, 9, 34093-34100.	8.0	23
105	Dual-layer vermiculite nanosheet based hybrid film to suppress dendrite growth in lithium metal batteries. Journal of Energy Chemistry, 2022, 69, 205-210.	12.9	23
106	Facile synthesis and photoelectrochemical characterization of Sb2O3 nanoprism arrays. Journal of Alloys and Compounds, 2017, 727, 469-474.	5.5	22
107	Thermal-evaporated selenium as a hole-transporting material for planar perovskite solar cells. Solar Energy Materials and Solar Cells, 2018, 185, 130-135.	6.2	22
108	One-step electrodeposition of CuGaSe2 thin films. Thin Solid Films, 2012, 520, 2781-2784.	1.8	21

#	Article	IF	CITATIONS
109	Impact of rapid thermal annealing of Mo coated soda lime glass substrate on device performance of evaporated Cu2ZnSnS4 thin film solar cells. Materials Letters, 2014, 125, 40-43.	2.6	20
110	The electrochemical self-assembly of hierarchical dendritic Bi2Se3 nanostructures. CrystEngComm, 2014, 16, 2823.	2.6	20
111	Back contact-absorber interface modification by inserting carbon intermediate layer and conversion efficiency improvement in Cu ₂ ZnSn(S,Se) ₄ solar cell. Physica Status Solidi - Rapid Research Letters, 2015, 9, 687-691.	2.4	20
112	Light-Bias-Dependent External Quantum Efficiency of Kesterite Cu2ZnSnS4 Solar Cells. ACS Photonics, 2017, 4, 1684-1690.	6.6	20
113	Graphene-Sb2Se3 thin films photoelectrode synthesized by in situ electrodeposition. Materials Letters, 2018, 224, 109-112.	2.6	20
114	Famatinite Cu ₃ SbS ₄ nanocrystals as hole transporting material for efficient perovskite solar cells. Journal of Materials Chemistry C, 2018, 6, 7989-7993.	5.5	20
115	Boosting the Electrochemical Performance of Allâ€Solidâ€State Batteries with Sulfide Li ₆ PS ₅ Cl Solid Electrolyte Using Li ₂ WO ₄ â€Coated LiCoO ₂ Cathode. Advanced Materials Interfaces, 2021, 8, 2100624.	3.7	20
116	In situ prepared Cu2ZnSnS4 ultrathin film counter electrode in dye-sensitized solar cells. Materials Letters, 2014, 121, 241-243.	2.6	19
117	CsPbl _{2.69} Br _{0.31} solar cells from low-temperature fabrication. Materials Chemistry Frontiers, 2019, 3, 1139-1142.	5.9	19
118	High-performance wide-bandgap copolymers with dithieno[3,2- <i>b</i> :2′,3′- <i>d</i>]pyridin-5(4 <i>H</i>)-one units. Materials Chemistry Frontiers, 2019, 3, 399-402.	5.9	18
119	A comprehensive hydrometallurgical recycling approach for the environmental impact mitigation of EoL solar cells. Journal of Environmental Chemical Engineering, 2021, 9, 106830.	6.7	17
120	Pulse-plating electrodeposition and annealing treatment of CuInSe2 films. Transactions of Nonferrous Metals Society of China, 2008, 18, 884-889.	4.2	16
121	Colloidal synthesis of Cu 2 FeSnSe 4 nanocrystals for solar energy conversion. Materials Letters, 2014, 136, 306-309.	2.6	16
122	Cu2ZnSnS4 thin film solar cells from coated nanocrystals ink. Journal of Materials Science: Materials in Electronics, 2015, 26, 1932-1939.	2.2	16
123	Realization of nanostructured N-doped p-type Bi 2 O 3 thin films. Materials Letters, 2017, 193, 228-231.	2.6	16
124	Fabrication of Efficient Cu2ZnSnS4 Solar Cells by Sputtering Single Stoichiometric Target. Coatings, 2017, 7, 19.	2.6	16
125	Template-directed synthesis of ordered iron pyrite (FeS2) nanowires and nanotubes arrays. Journal of Sol-Gel Science and Technology, 2014, 72, 100-105.	2.4	15
126	Fabrication of Cu2ZnSnS4 thin film solar cells by sulfurization of electrodeposited stacked binary Cu–Zn and Cu–Sn alloy layers. Materials Letters, 2015, 155, 44-47.	2.6	15

#	Article	IF	CITATIONS
127	The electrochemical behavior of tellurium on stainless steel substrate in alkaline solution and the illumination effects. Journal of Electroanalytical Chemistry, 2016, 771, 17-22.	3.8	15
128	Fabrication of Cu2ZnSnS4 thin film solar cells by annealing of reactively sputtered precursors. Journal of Alloys and Compounds, 2017, 701, 55-62.	5.5	15
129	Amorphous Sb 2 S 3 Anodes by Reactive Radio Frequency Magnetron Sputtering for Highâ€Performance Lithiumâ€Ion Half/Full Cells. Energy Technology, 2019, 7, 1900928.	3.8	15
130	Regeneration of Al-doped LiNi0.5Co0.2Mn0.3O2 cathode material by simulated hydrometallurgy leachate of spent lithium-ion batteries. Transactions of Nonferrous Metals Society of China, 2022, 32, 593-603.	4.2	15
131	Photoelectrochemical Behavior of Electrodeposited CoSe Thin Films. Applied Physics Express, 2011, 4, 071201.	2.4	14
132	Thermodynamic analysis on metal selenides electrodeposition. Journal of Alloys and Compounds, 2013, 557, 40-46.	5.5	14
133	Fabrication of earth-abundant Cu ₂ ZnSn(S,Se) ₄ light absorbers by a sol–gel and selenization route for thin film solar cells. RSC Advances, 2016, 6, 6562-6570.	3.6	14
134	Hybrid Ag Nanowire–ITO as Transparent Conductive Electrode for Pure Sulfide Kesterite Cu ₂ ZnSnS ₄ Solar Cells. Journal of Physical Chemistry C, 2017, 121, 20597-20604.	3.1	14
135	Preparation of Sb2O3/Sb2S3/FeOOH composite photoanodes for enhanced photoelectrochemical water oxidation. Transactions of Nonferrous Metals Society of China, 2020, 30, 1625-1634.	4.2	14
136	Sb2S3 nanorods/porous-carbon composite from natural stibnite ore as high-performance anode for lithium-ion batteries. Transactions of Nonferrous Metals Society of China, 2021, 31, 2051-2061.	4.2	14
137	Sol-gel solution-processed Cu2SrSnS4 thin films for solar energy harvesting. Thin Solid Films, 2020, 697, 137828.	1.8	14
138	Al/Pb lightweight grids prepared by molten salt electroless plating for application in lead-acid batteries. Journal of Power Sources, 2014, 256, 294-300.	7.8	13
139	Transmission electron microscopy analysis for the process of crystallization of \$ext{C}{{ext{u}}_{2}}ext{ZnSn}{{ext{S}}_{4}}\$ film from sputtered Zn/CuSn precursor. Nanotechnology, 2014, 25, 195701.	2.6	13
140	In situ growth of CuSbS2 thin films by reactive co-sputtering for solar cells. Materials Science in Semiconductor Processing, 2018, 84, 101-106.	4.0	13
141	Rapid sintering of ceramic solid electrolytes LiZr2(PO4)3 and Li1.2Ca0.1Zr1.9(PO4)3 using a microwave sintering process at low temperatures. Ceramics International, 2019, 45, 11068-11072.	4.8	13
142	Transition metal dichalcogenides in alliance with Ag ameliorate the interfacial connection between Li anode and garnet solid electrolyte. Journal of Power Sources, 2020, 468, 228379.	7.8	13
143	Synergistic defect- and interfacial-engineering of a Bi ₂ S ₃ -based nanoplate network for high-performance photoelectrochemical solar water splitting. Journal of Materials Chemistry A, 2022, 10, 7830-7840.	10.3	13
144	Effects of hydrogen peroxide on electrodeposition of Cu(In,Ga)Se 2 thin films and band gap controlling. Electrochimica Acta, 2014, 142, 208-214.	5.2	12

#	Article	IF	CITATIONS
145	Nanoscale interface engineering of inorganic Solid-State electrolytes for High-Performance alkali metal batteries. Journal of Colloid and Interface Science, 2022, 621, 41-66.	9.4	12
146	Structural and Optical Properties of Electrodeposited Bi2-xSbxSe3 Thin Films. ECS Solid State Letters, 2012, 1, Q29-Q31.	1.4	11
147	Spatial Grain Growth and Composition Evolution during Sulfurizing Metastable Wurtzite Cu ₂ ZnSnS ₄ Nanocrystal-Based Coatings. Chemistry of Materials, 2017, 29, 2110-2121.	6.7	11
148	Colloidal synthesis and characterization of single-crystalline Sb ₂ Se ₃ nanowires. RSC Advances, 2017, 7, 24589-24593.	3.6	11
149	Characterization of Bi2S3 thin films synthesized by an improved successive ionic layer adsorption and reaction (SILAR) method. Materials Letters, 2017, 209, 479-482.	2.6	11
150	Low ost Fabrication of Sb ₂ S ₃ Solar Cells: Direct Evaporation from Raw Stibnite Ore. Solar Rrl, 2022, 6, .	5.8	11
151	Preparation and characterization of Bi2Se3 nanowires by electrodeposition. Electrochimica Acta, 2011, 56, 5085-5089.	5.2	10
152	Hot-injection synthesis of Co0.85Se nanocrystals for photo-electrical application. Materials Letters, 2013, 108, 110-113.	2.6	10
153	CuSbS2 Nanocrystals Applying in Organic-Inorganic Hybrid Photodetectors. ECS Solid State Letters, 2014, 3, Q41-Q43.	1.4	10
154	Cu2ZnSnS4 thin film solar cell fabricated by co-electrodeposited metallic precursor. Journal of Materials Science: Materials in Electronics, 2015, 26, 204-210.	2.2	10
155	Shape and stoichiometry control of bismuth selenide nanocrystals in colloidal synthesis. RSC Advances, 2016, 6, 47840-47843.	3.6	10
156	Sb ₂ O ₃ /Sb ₂ S ₃ Heterojunction Composite Thin Film Photoanode Prepared via Chemical Bath Deposition and Post-Sulfidation. Journal of the Electrochemical Society, 2018, 165, H1052-H1058.	2.9	10
157	Hydrogen evolution behavior of aluminum cathode in comparison with stainless steel for electrowinning of manganese in sulfate solution. Hydrometallurgy, 2018, 179, 245-253.	4.3	10
158	Catalytic effects of NH4+ on hydrogen evolution and manganese electrodeposition on stainless steel. Transactions of Nonferrous Metals Society of China, 2019, 29, 2430-2439.	4.2	10
159	Carbon quantum dots sensitized Bi2O3 photoanode with enhanced photoelectrocatalytic properties. Chemical Physics Letters, 2020, 739, 137025.	2.6	9
160	Effects of Cu/In ratio of electrodeposited precursor on post-sulfurization process in fabricating quaternary CuIn(S,Se)2 thin films. Applied Surface Science, 2011, 257, 8360-8365.	6.1	8
161	Improving the crystallization and carrier recombination of Cu2ZnSnS4 thin film deposited on Mo-coated soda-lime glass by extra sodium doping through solution process. Materials Letters, 2019, 254, 50-53.	2.6	8
162	Bi ₂ O _{2.33} Nanostructure-Based Photoanodes for Photoelectrochemical Determination of Trace Soluble Sulfides. ACS Applied Nano Materials, 2021, 4, 5778-5784.	5.0	8

#	Article	IF	CITATIONS
163	Sulfurized polyacrylonitrile cathodes with electrochemical and structural tuning for high capacity all-solid-state lithium–sulfur batteries. Sustainable Energy and Fuels, 2021, 5, 5603-5614.	4.9	8
164	Electrodeposition-Based Preparation of Cu(In,Ga)(Se,S)[sub 2] Thin Films. Electrochemical and Solid-State Letters, 2009, 12, D65.	2.2	7
165	Preparation and Characterization of AgSbSe ₂ Thin Films by Electrodeposition. Journal of the Electrochemical Society, 2013, 160, D578-D582.	2.9	7
166	Optimization of precursor deposition for evaporated Cu2ZnSnS4 solar cells. Applied Physics A: Materials Science and Processing, 2015, 118, 893-899.	2.3	7
167	Study on the adhesive mechanism between the Ga doped ZnO thin film and the polycarbonate substrate. Materials Science in Semiconductor Processing, 2017, 66, 105-108.	4.0	7
168	Study on the Adhesion Force Between Ga-Doped ZnO Thin Films and Polymer Substrates. Journal of Nanoscience and Nanotechnology, 2019, 19, 240-244.	0.9	7
169	Enhancing the performance of Cu2ZnSnS4 solar cell fabricated via successive ionic layer adsorption and reaction method by optimizing the annealing process. Solar Energy, 2021, 220, 204-210.	6.1	7
170	Perovskite Quantum Dot Solar Cells Fabricated from Recycled Lead-Acid Battery Waste. , 2022, 4, 120-127.		7
171	Room-temperature deposition of flexible transparent conductive Ga-doped ZnO thin films by magnetron sputtering on polymer substrates. Journal of Materials Science: Materials in Electronics, 2017, 28, 6093-6098.	2.2	6
172	Effects of Illumination on the Electrochemical Behavior of Selenium Electrodeposition on ITO Substrates. Journal of the Electrochemical Society, 2017, 164, H225-H231.	2.9	6
173	Electrochemical behavior simulation of high specific energy power lithium-ion batteries based on numerical model. Ionics, 2020, 26, 5513-5523.	2.4	6
174	A Green Lead Recycling Strategy from Used Lead Acid Batteries for Efficient Inverted Perovskite Solar Cells. Journal of Physical Chemistry Letters, 2021, 12, 9595-9601.	4.6	6
175	Preparation and Characterization of Co-Se Thin Films by Electrodeposition. Wuji Cailiao Xuebao/Journal of Inorganic Materials, 2011, 26, 403-410.	1.3	6
176	Cu ₂ Si _{<i>x</i>} Sn _{1â^'<i>x</i>} S ₃ Thin Films Prepared by Reactive Magnetron Sputtering For Low-Cost Thin Film Solar Cells. Chinese Physics Letters, 2011, 28, 108801.	3.3	5
177	Photoelectrochemical Deposition of CuInSe2 Thin Films. Electrochemical and Solid-State Letters, 2012, 15, D19.	2.2	5
178	Improvement of Mo/Cu2ZnSnS4 interface for Cu2ZnSnS4 (CZTS) thin film solar cell application. Materials Research Society Symposia Proceedings, 2014, 1638, 1.	0.1	5
179	Fabrication of Cu 2 ZnSn(S,Se) 4 thin film solar cells by selenization of reactively sputtered precursors. Materials Letters, 2016, 182, 336-339.	2.6	5

180 Towards 9% sulfide CZTS solar cells fabricated by a sol-gel process. , 2018, , .

#	Article	IF	CITATIONS
181	The effect of different Cu/Sn ratios on the properties of monoclinic Cu2SnS3 thin films and solar cells fabricated by the sol–gel method. Journal of Materials Science: Materials in Electronics, 2019, 30, 4378-4384.	2.2	4
182	Large Voc improvement and 9.2% efficient pure sulfide Cu <inf>2</inf> ZnSnS <inf>4</inf> solar cells by heterojunction interface engineering. , 2016, , .		3
183	Understanding the effect of Cadmium alloying in high-efficiency sulphide kesterite Cu2ZnxCd1-xSnS4 solar cell by PDS and HRSTEM. , 2018, , .		3
184	Effect of sulfurization temperature on the properties of Culn(S,Se)2 thin films fabricated from electrodeposited CulnSe2 precursors. Superlattices and Microstructures, 2018, 122, 614-623.	3.1	3
185	Cyclic Voltammetry Analysis of Co-Electrodeposition Mechanism of rGO-Sb ₂ Se ₃ Thin Films Photocathode. Journal of the Electrochemical Society, 2019, 166, D421-D426.	2.9	3
186	Ultra-fine Sb2S3 particles encapsulated in activated-carbon: A high-performance anode for Li-ion batteries. Journal of Alloys and Compounds, 2022, 907, 164469.	5.5	3
187	The integration structure enhances performance of perovskite solar cells. Science Bulletin, 2021, 66, 310-313.	9.0	2
188	11.39% efficiency Cu ₂ ZnSn(S,Se) ₄ solar cells from scrap brass. SusMat, 2022, 2, 206-211.	14.9	2
189	Cu ₂ ZnSnS ₄ thin film solar cell fabricated by magnetron sputtering and sulfurization. Materials Research Society Symposia Proceedings, 2014, 1638, 1.	0.1	1
190	Anode Electrolysis of Manganese Dioxide in Photoelectrochemical Cells. Jom, 2021, 73, 2479.	1.9	1
191	Magnetron sputtering Al–Sc alloying layer gifts long cycle life for lithium metal batteries. Materials Letters, 2021, 294, 129705.	2.6	1
192	Structure and Electrical Property of CuInS ₂ Thin Films Deposited by DC Reactive Magnetron Sputtering. Wuji Cailiao Xuebao/Journal of Inorganic Materials, 2011, 26, 1287-1292.	1.3	1
193	Characterization of CuInS <inf>2</inf> thin films prepared by one-step DC reactive sputtering. , 2009, , .		0
194	Transmission electron microscopy analysis of secondary phases in Cu2ZnSnS4 thin film solar cells. Materials Research Society Symposia Proceedings, 2014, 1670, 83.	0.1	0
195	Dynamic analysis on metal selenide electrodeposition. Journal of Solid State Electrochemistry, 2014, 18, 1833-1845.	2.5	0
196	Synthesis of Cu2ZnSnS4 thin film from mixed solution of Cu2SnS3 nanoparticles and Zn ions. Transactions of Nonferrous Metals Society of China, 2016, 26, 2102-2108.	4.2	0
197	Towards 10% State-of-the-Art Pure Sulfide Cu2ZnSnS4 Solar Cell by modifying the Interface Chemistry. , 2017, , .		0
198	ALD ZnSnO buffer layer for enhancing heterojunction interface quality of CZTS solar cells. , 2018, , .		0

#	Article	IF	CITATIONS
199	Boosting the efficiency of kesterite Cu2ZnSnS4 solar cells by optimizing the heterojunction interface quality. , 2018, , .		0
200	Solution-processed ultrathin SnO2 passivation of Absorber/Buffer Heterointerface and Grain Boundaries for High Efficiency Kesterite Cu2ZnSnS4 Solar Cells. , 2019, , .		0
201	Kesterite Cu ₂ ZnSnS _{4-x} Se _x Thin Film Solar Cells. , 0, , .		0